Paleoseismicity of the Alamogordo fault along the Sacramento Mountains, southern Rio Grande rift, New Mexico

D. J. Koning and F. J. Pazzaglia

2002, pp. 107-119. https://doi.org/10.56577/FFC-53.107

in:

Geology of White Sands, Lueth, Virgil; Giles, Katherine A.; Lucas, Spencer G.; Kues, Barry S.; Myers, Robert G.; Ulmer-Scholle, Dana; [eds.], New Mexico Geological Society 53rd Annual Fall Field Conference Guidebook, 362 p. https://doi.org/10.56577/FFC-53

This page is intentionally left blank to maintain order of facing pages.

New Mexico Geological Society Guidebook, 53rd Field Conference, Geology of White Sands, 2002, p. 107-119.

PALEOSEISMICITY OF THE ALAMOGORDO FAULT ALONG THE SACRAMENTO MOUNTAINS, SOUTHERN RIO GRANDE RIFT, NEW MEXICO

D. J. KONING[1] AND F. J. PAZZAGLIA[2]

[1]14193 Henderson Dr., Rancho Cucamonga, CA 91739; danchikoning@yahoo.com; [2]Lehigh University, Department of Earth and Environmental Sciences, 31 Williams Dr., Bethlehem, PA 18015; fjp3@lehigh.edu

ABSTRACT.—The Alamogordo fault of the southern Rio Grande rift, New Mexico, is a major rift-bounding structure that has down-dropped the Tularosa Basin on the west relative to the Sacramento Mountains on the east. The distribution of late Quaternary rupture activity of the Alamogordo fault adjacent to the Sacramento Mountains was investigated by measuring fault scarp profiles at 40 localities, mapping proximal piedmont deposits, and describing and dating exposures of offset Quaternary sediment.

The timing of four late Quaternary surface rupture events is constrained by stratigraphic relationships and C-14 radiometric determinations. An additional older, poorly constrained event possibly happened at about 20-30 ka. The two older of the four constrained rupture events probably occurred within a time span of 1000-2000 years before 12,600 (radiocarbon years). The estimated average displacement for these two events is 1-3 m. North of the city of Alamogordo, the youngest interpreted surface rupture event occurred between 10,500 and 11,300 radiocarbon years. South of Alamogordo, the youngest surface rupture likely occurred in the early Holocene during a period of major alluvial fan aggradation. This event probably had an average displacement of 0.5 to1 m. The difference in the timing of the youngest surface rupture event relative to location supports the interpretation that the southern Alamogordo fault consists of two segments, with the common segment boundary located near Alamogordo. Based on empirical length-displacement-magnitude relations, the four constrained ruptures are estimated to have been associated with ancient earthquakes having seismic moment magnitudes of 6.7 to 7.3.

INTRODUCTION

The Alamogordo fault is a major feature of the Rio Grande rift in south-central New Mexico that defines the structural boundary between the Tularosa Basin and the Sacramento Mountains, along which the latter have been uplifted (Fig. 1). This normal fault extends 110 km end-to-end (134 km-long trace: Machette et al., 1998) along the eastern margin of the Tularosa Basin, and has displaced surfaces developed on Quaternary deposits by as much as 10 m. A significant portion of the fault lies within 20 km of the city of Alamogordo and the Holloman Air Force Base. The timing of late Quaternary rupture events along 60 km of the Alamogordo fault, adjacent to the Sacramento Mountains, was investigated by: (1) measuring fault scarp profiles at 40 localities, (2) mapping proximal piedmont deposits along the western foot of the Sacramento Mountains, and (3) describing exposures of offset Quaternary sediment and collecting 11 samples of dateable material. This paper describes the results of these three procedures and discusses seismic risk implications for the Alamogordo region.

STUDY AREA

The study area is along the central-eastern margin of the Tularosa Basin, New Mexico, and includes alluvial fans deposited from mountain-front canyons incised into the Paleozoic strata of the Sacramento Mountains (Fig. 1). The study area extends from Coyote Canyon southward to Negro Ed Canyon (about 60 km long and 30 km wide). Within this area, 37 linear km of the proximal piedmont (the piedmont closest to the mountain front) was investigated in detail and mapped at a scale of 1:24,000 (Fig. 1).

PREVIOUS WORK

Both Otte (1959) and Pray (1961) noted that the Sacramento Mountains were uplifted along a range-bounding fault zone. Kelley and Thompson (1964) showed a fault separating the Sacramento Mountains from the Tularosa Basin on their tectonic map and labeled it the "Sacramento fault." Machette (1987a) renamed the Sacramento fault (*sensu* Kelley and Thompson, 1964) the "Alamogordo fault" and found evidence for two possible rupture events in the latest Pleistocene or Holocene (<30 ka) based on analysis of 13 fault scarp profiles. Machette et al. (1998) divided the Alamogordo fault into three sections; the middle section is called the "Sacramento section" and generally corresponds to the 60 km of the fault in the study area.

TIMING OF PAST RUPTURE EVENTS

Fault Scarp Profile Data

Topographic profiles of fault scarps were measured at 40 localities (FSP-1 through FSP-40) in the study area using an electronic theodolite (also known as a Total Station) or a tape and abney level. Profile attributes that can be measured from fault scarps are shown in Figure 2; a complete listing of fault scarp morphometric data is in Koning (1999). Alamogordo fault scarp heights average 6-7 m (range of 2-13 m), and surface offsets average about 5 m (range of 1-10 m). We plot the maximum midslope angle as a function of the scarp height, following methods of Bucknam and Anderson (1979), and also plot the slope vs. the height of significant steep bevels on the scarp (Fig. 3). Comparison of the data to regression lines of the Holocene Organ Mountains fault scarp (Machette, 1987a), 60-80 km to the southwest, and to a dated Lake Bonneville shoreline (Oviatt et al., 1992) suggests that the youngest (i.e., steepest) bevel of compound scarps formed in the Holocene. Aside from this steepest bevel, the fault scarp data generally plot on or just above the 14.5 ka Lake Bonneville shoreline regression line.

Maximum fault scarp heights are generally 3-6 m lower north of the Indian Wells mountain-front reentrant compared to the

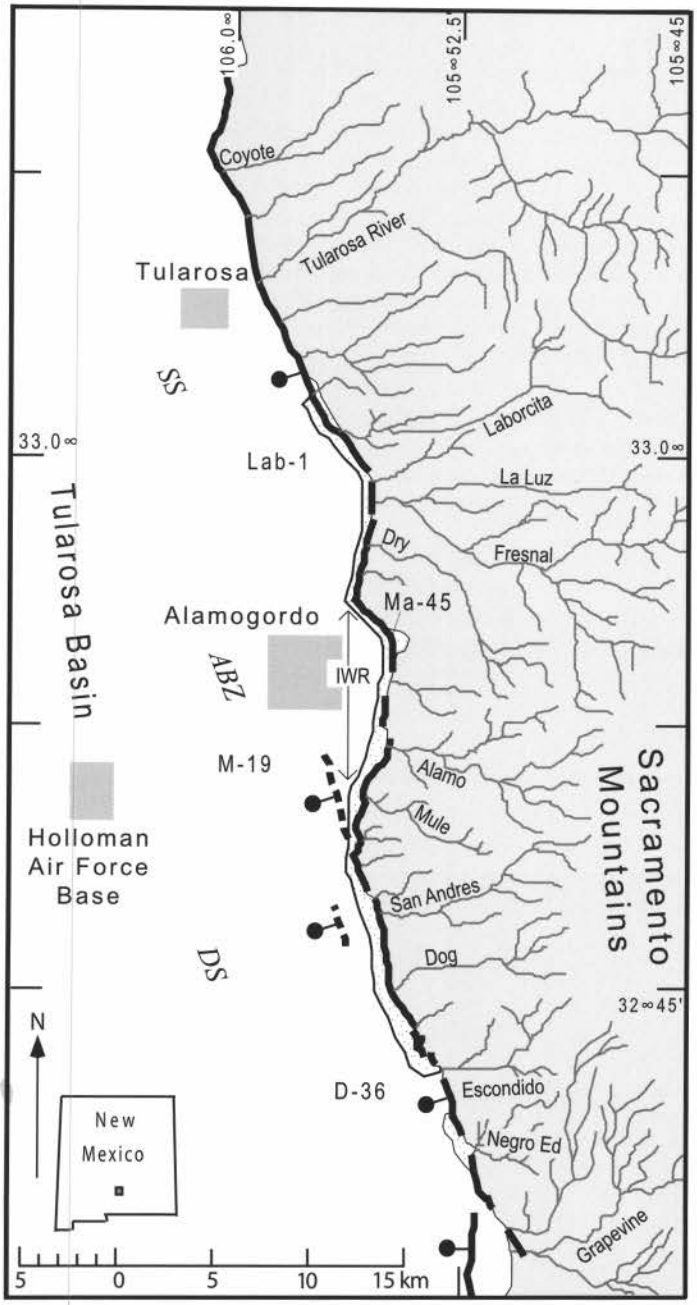

FIGURE 1. Map of study area. Sacramento Mountains are shown by shaded area and canyons draining their west front are labeled. Stippled area is the approximate extent of proximal alluvial fans that were mapped along 37 km of the mountain front (refer to Koning, 1999, for more detail of mapped area). Key sites discussed in text are labeled (e.g., Lab-1, M-19). Location of site Ma-45 is N: 3,642,120±30 m, E: 413,950±30 m (UTM zone 13, NAD 27). Location of Alamogordo fault is based on mapping of Koning (1999) and Michael Machette (pers. comm., 1997) and is shown by the bold black line (solid where depicted by fault scarps; short dashes mark approximate location of subsurface faults). Interpreted fault segments are: SS = Sabinata Segment, ABZ=Alamogordo Boundary Zone, DS=Deadman Segment. IWR = Indian Wells mountain-front reentrant.

fault scarps to the south (Koning, 1999, fig. 39). This is consistent with our interpretation (discussed below) that two fault segments are present in the study area. The northern segment is called the Sabinata segment, and the southern segment is called the Deadman segment (Fig. 1). Outside of the study area, however, other segments likely exist along the Alamogordo fault; these other segments may correspond to the Three Rivers and McGregor sections of Machette et al. (1998).

Alluvial Fan Stratigraphy of the Piedmont West of the Southern Sacramento Mountains

Fault scarps were confidently identified only in the proximal regions of the alluvial fans, so mapping and descriptive efforts were focused there. Textural classification of gravelly alluvium follows Folk (1954). Soil nomenclature and descriptions follow the Soil Survey Staff (1992) and Birkeland (1999); abbreviations of soil properties are listed in Koning et al. (this volume, table 1).

The alluvial-fan deposits in the study area generally consist of poorly to moderately sorted, subangular to subrounded, silty-sandy gravel derived from the Sacramento Mountains. Three alluvial fan depositional units can be distinguished and mapped based on sedimentologic and spatial (e.g., inset) relationships; these are labeled Qf1, Qf2, and Qf3, from oldest to youngest (Fig. 4; Koning et al., this volume, table 2). These three units also have unique surficial and soil characteristics that were used as mapping criteria where exposures are lacking (Koning, 1999). Another unit, Qfoi, represents older inset gravel intermediate in age between Qf1 and Qf2; this unit is buried, only recognized at two exposures, and was not mapped — which is why we give it a unique label. These units are more thoroughly discussed in Koning et al. (this volume). Complete descriptive data of units Qf1 through Qf3, plus two older pediment-associated deposits, are found in Koning (1999).

The oldest alluvial-fan unit, Qf1, is more than 10 m thick and commonly extends into the lower reaches of mountain canyons as a thick fill. Unit Qf1 is generally considered to be late Pleistocene to late middle(?) Pleistocene in age (25-300? ka) based on two C-14 dates, its strong soil development (calcic horizons have stage II+ to IV carbonate morphology), and sedimentologic and pedologic similarities with the Jornada II and Camp Rice piedmont facies alluvium near Las Cruces (Koning et al., this volume).

Unit Qfoi is present locally at the mouths of mountain front canyons, where it appears to be inset against older Qf1 sediment and buried by younger sediment (Fig. 4). The unit is interpreted to be latest Pleistocene in age (10-25 ka), and it may represent a period of time when alluvial fans in the study area were entrenched (Koning et al., this volume). Some inset terrace surfaces that are locally preserved on top of unit Qf1 (Fig. 5) may possibly have formed during the early stages of latest Pleistocene incision associated with unit Qfoi.

Qf2 deposits are 2-5 m thick, may overlie Qf1 deposits downstream of large fault scarps, and tend to be inset into Qf1 deposits upstream of large fault scarps (Fig. 4). The age of unit Qf2 is interpreted to be early Holocene based on three C-14 dates and similarities of its soil with the soil developed on Isaacks' Ranch alluvium near Las Cruces (Koning et al, this volume). The lower,

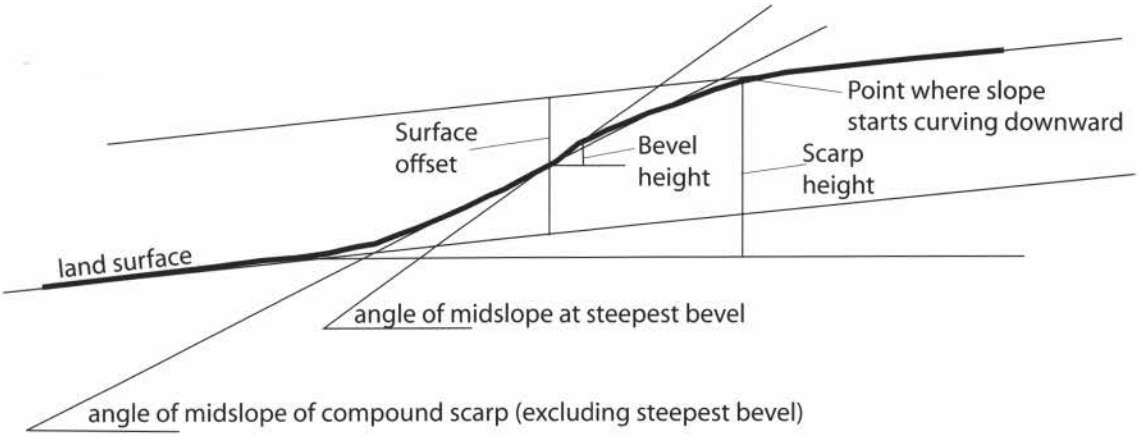

FIGURE 2. Diagram illustrating various fault scarp profile measurements.

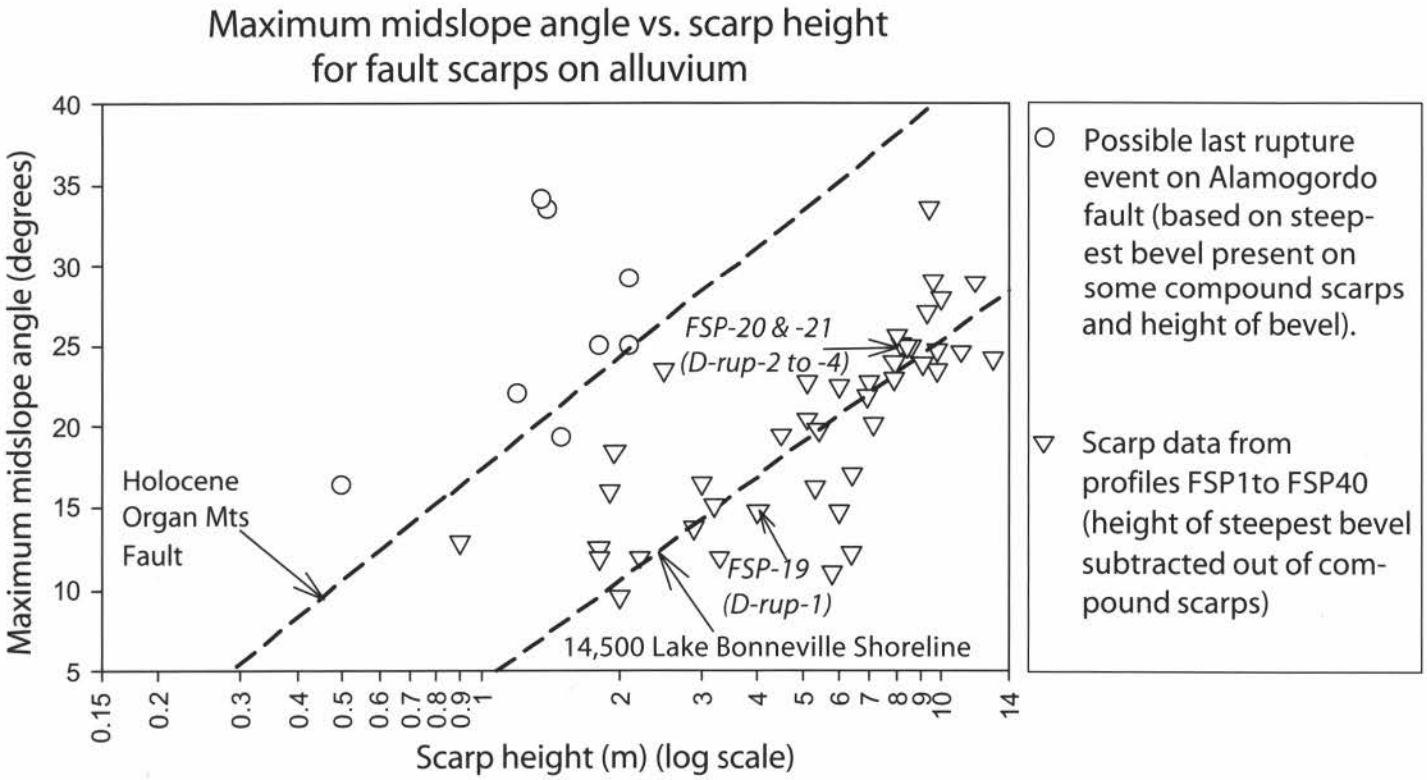

FIGURE 3. Plot demonstrating fault scarp morphology derived from profiles FSP-1 through FSP-40 (Koning, 1999). Note that most of the data lie on or just above the 14,500 (^{14}C yrs B.P., not calibrated) Lake Bonneville shoreline regression (age of shoreline from Oviatt et al., 1992; regression from Bucknam and Anderson, 1979). The plotted position of the data agrees with stratigraphic and chronologic data that indicate two big rupture events occurred within about 2,000 years prior to 12,600 (^{14}C yrs B.P.). Data from site L-13 are delineated. Note that the older scarp (FSP-19) lies below the 14.5 ka Bonneville regression line and the two younger scarps (FSP-20 and 21) lie just above.

older portions of Qf2 deposits are observed to have been offset 0.5 to 1 m by the Alamogordo fault, but the resulting scarps were generally buried or removed by upper Qf2-related deposition (sites D-36 and Ma-45; Figs. 1 and 6).

Unit Qf3 is commonly inset into Qf1 and Qf2 near the mountain front and overlies these older units in the medial and distal regions of the alluvial fans (Fig. 4). Unit Qf3 is 1-2 m thick and not offset by the Alamogordo fault. Soil, stratigraphic, and surface characteristics of Qf3 are consistent with a mid to late Holocene age (Koning et al., this volume).

Implications for Late Quaternary Paleoseismicity Based on Alluvial Fan Stratigraphic Relationships

Mapping and dating of alluvial-fan deposits and measurements of their respective displacements allow us to reconstruct

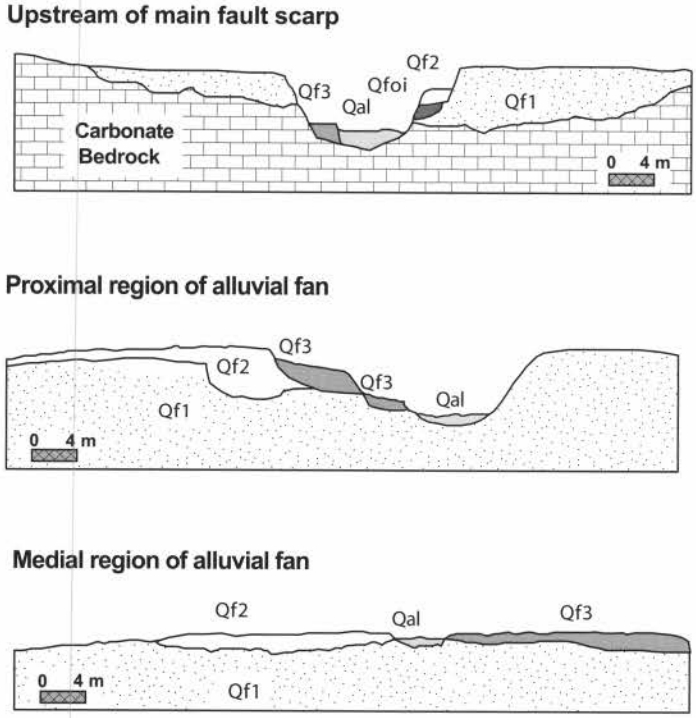

FIGURE 4. Schematic representation of alluvial-fan stratigraphy along the western front of the Sacramento Mountains.

the chronology of past rupture events along the studied part of the Alamogordo fault. The late Pleistocene Qf1 surface is offset by as much as 10 m south of Alamogordo (Koning, 1999). In contrast, the Qf2 surface is generally not offset where it overlies the Alamogordo fault, although south and east of Alamogordo basal Qf2 deposits may be offset by 0.5-1 m (Fig. 6). No offset of unit Qf3 has been observed. Thus, substantial offset has occurred along the Alamogordo fault during the latest Pleistocene – after the stabilization of most of the Qf1 surface (interpreted to have generally occurred prior to 25 ka) but before the early Holocene deposition of unit Qf2. The youngest rupture event (called D-rup-4; the "D" refers to the Deadman segment) occurred east and south of Alamogordo during early Holocene deposition of unit Qf2 (Fig. 7).

The oldest rupture event (D-rup-1) is locally recognized by a ~4 m high fault scarp (2.4 m of surface offset) that has formed on an older Qf1 surface but does not extend across a younger inset surface on unit Qf1 (Fig. 5). The younger surface has a calcic soil with weak stage III carbonate morphology (Koning, 1999, appendix D), and it may have formed either during the early stages of inferred latest Pleistocene fan incision or perhaps earlier. Accordingly, the oldest observed rupture event is probably older than 20 ka; however, its scarp morphology appears consistent with a latest Pleistocene rupture event (Fig. 3). Thus, our best age estimate for this oldest event is 20-30 ka (Fig. 7). A younger, 8 m-tall fault scarp (6.0-6.3 m of surface offset) to the east has formed on both of these Qf1 surfaces and clearly post-dates the western, 4-m tall fault scarp (Fig. 5). The bulk of this younger fault scarp was probably formed by ruptures D-rup-2 and D-rup-3, which are discussed below. Evidence for a separate rupture event on the Sabinata segment (S-rup-1) is discussed in the following.

Exposures of Faulted Quaternary Sediment

Nine exposures of faulted Quaternary sediment were sketched, described, and sampled for material that could be radiometrically dated. Beta Analytic Inc. performed all C-14 radiometric dating analyses, and sample numbers listed below are from this laboratory. Fault-scarp colluvium was locally subdivided into architectural elements following Nelson (1992) (Fig. 8 and Table 1); these elements have genetic and temporal significance and are thus useful for paleoseismic studies. Two exposures proved particularly useful and are briefly described below; complete descriptions are given in Koning (1999).

Site Lab-1

Description:
Site Lab-1 is a road cut on the north wall of Laborcita Arroyo where the arroyo exits the mountains (Figs. 1 and 9). On the footwall, Qf1 deposits are primarily a reddish yellow, silty very fine to fine sand with minor lenticular, 10-30-cm-thick, pebble beds. The upper part of the footwall is not exposed. In the hanging wall, the sediment is a light brown, clast-supported, sandy gravel that appears to comprise a channel fill correlative to unit Qfoi. Two calcic soils, each marked by stage I carbonate morphology and distinct clay films, have developed on the upper meter of the hanging wall Qfoi alluvium. Radiocarbon analyses of charcoal collected from the upper soil (sample Beta-120931) yielded a date of 11,240 ± 70 radiocarbon years before present (hereafter abbreviated as ^{14}C yrs B.P. and cited throughout text with 1-sigma errors).

Four separate colluvial units are identified and labeled C1 through C4 (oldest to youngest) (Fig. 9). C1 is wedge-shaped and consists of light brown, clast-supported gravel. Carbonate covers ~20% of clast surfaces in <0.2 mm-thick coats that are broken and chipped. C2 is composed of light brown, matrix- and clast-supported gravel and has a wedge shape. C3 is matrix-supported and has a darker color than C1 and C2 (brown as opposed to light brown), a 10 m-long lenticular shape, and only 10-15% gravel. Radiocarbon analyses of gastropods in this unit returned a date of 10,510 ± 40 ^{14}C yrs B.P. (sample Beta-125266), but radiocarbon analyses of charcoal returned a date of 13,650 ± 70 ^{14}C yrs B.P. (sample Beta-120932 – not shown on Figure 9). Unit C4 is tabular, unconformably overlies the older units, and composed of massive gravelly silt and clay with no internal sedimentary structures. A soil has developed on C4 that is marked by a stage I carbonate morphology and gypsum nodules.

Paleoseismic Interpretation:
Units C1 through C4 represent deposits of a single, non-deformed, one rupture event-related, colluvial package formed from erosion of a fault scarp. C1 and C2 are inferred to represent lower debris elements, C3 the upper debris element, and C4 the wash element of this fault scarp colluvium based on comparison

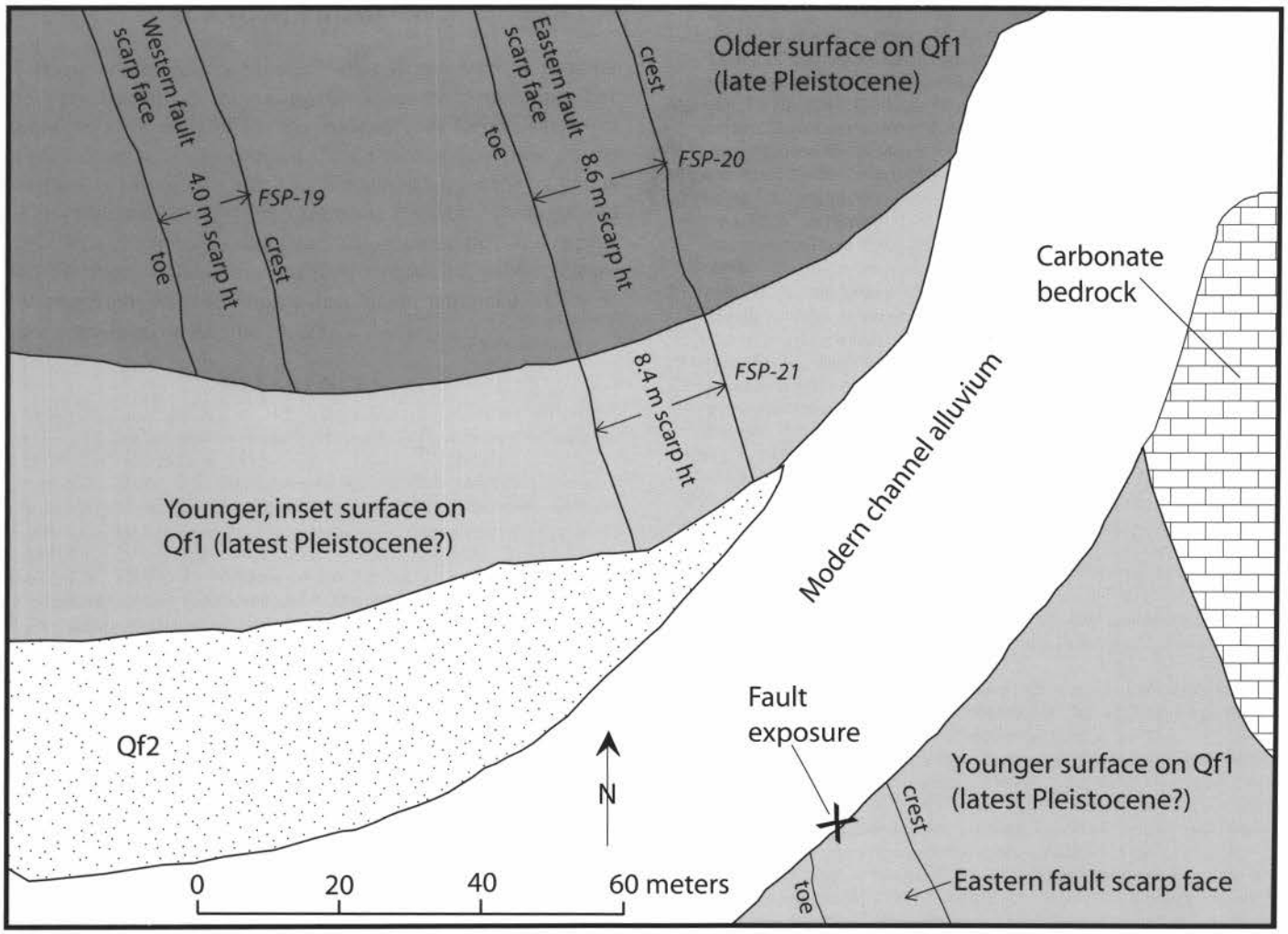

FIGURE 5. Map of site L-13 from total station survey in January, 1998; located 600 m south of Lead Canyon. Note the younger surface inset into an older surface developed on Qf1. An older 4 m tall fault scarp does not continue across this younger surface; this scarp marks the oldest inferred rupture event in the study area (D-rup-1). Locations of fault scarp profiles (FSP-19 to –21) are labeled.

of these units to characteristics listed in Table 1. In unit C3, the C-14 date of 10,510 ± 40 ^{14}C yrs B.P. from snail shells is preferred over the date of 13,650 ± 70 ^{14}C yrs B.P. from charcoal because the snail shells appear more fragile and less likely than charcoal to survive reworking from older sediment eroding out of the adjacent scarp face. Furthermore, the date of the shell preserves the stratigraphic order considering the underlying charcoal C-14 date of 11,240 ± 70 ^{14}C yrs B.P. The exposure records only the latest rupture event, which is interpreted to have occurred between 10,500 and 11,300 ^{14}C yrs B.P. This rupture event is referred to as S-rup-1 (Fig. 7) — the "S" in the label refers to the Sabinata fault segment.

Site M-19

Description:

Site M-19 is an excellent exposure more than 6 m in height that exhibits faulted alluvial and colluvial sediment (Fig. 10). The footwall is entirely composed of Qf1 alluvium. In the hanging wall, two Qf1 allostratigraphic units (A1 and A2) have been downwarped toward the southeast by motion along the fault. Unit A1 has a well developed, 170-200 cm thick soil mostly comprised of calcic horizons with carbonate morphologies as advanced as stage III+ carbonate morphology. Unit A2 is about 80-90 cm thick and has a soil with local calcic horizon(s) of stage II to II+ carbonate morphologies.

Near the fault zone there are two blocks of sediment whose bedding is near vertical due to rotation. A bed-by-bed descriptive comparison of the rotated blocks with unit A2 and the upper two-thirds of A1 is compellingly similar (Koning, 1999, appendix C). Thus, these rotated blocks are designated as units A1' and A2' (Fig. 10). Charcoal collected from deformed soil at the top of unit A2' was C-14 dated at 12, 990 ± 150 ^{14}C yrs B.P. (sample Beta-117015).

Colluvial units, designated as C1a through C2e, overlie units A1 and A2 (Fig. 10). Unit C1a is a clast-supported, poorly sorted, wedge-shaped unit composed of cobbles and pebbles in a sandy clay loam and clay loam matrix. Being about 1 m thick, unit C1a generally has no clast fabric, only vague horizontal bedding, and a sharp lower contact. A weak soil, marked by very few to few, faint to distinct, clay films and weak structural development has

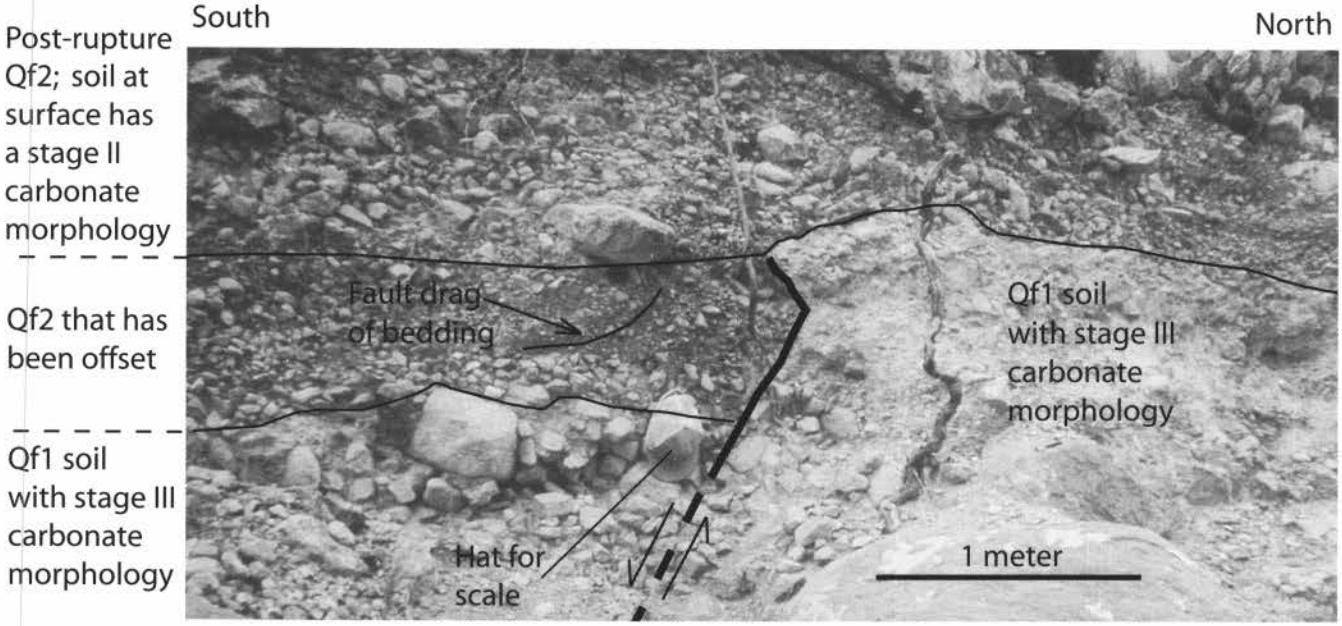

FIGURE 6. Photograph of Qf2 deposit at site D-36 (see Fig. 1). Alamogordo fault is shown by bold black line; dashed where covered. Relative fault motion is indicated by arrows. Another fault with 35 cm of offset is located 1-7 m to the right of this part of the exposure. Located at N: 3,620,450±30 m, E: 416,200±30 m (UTM zone 13, NAD 27).

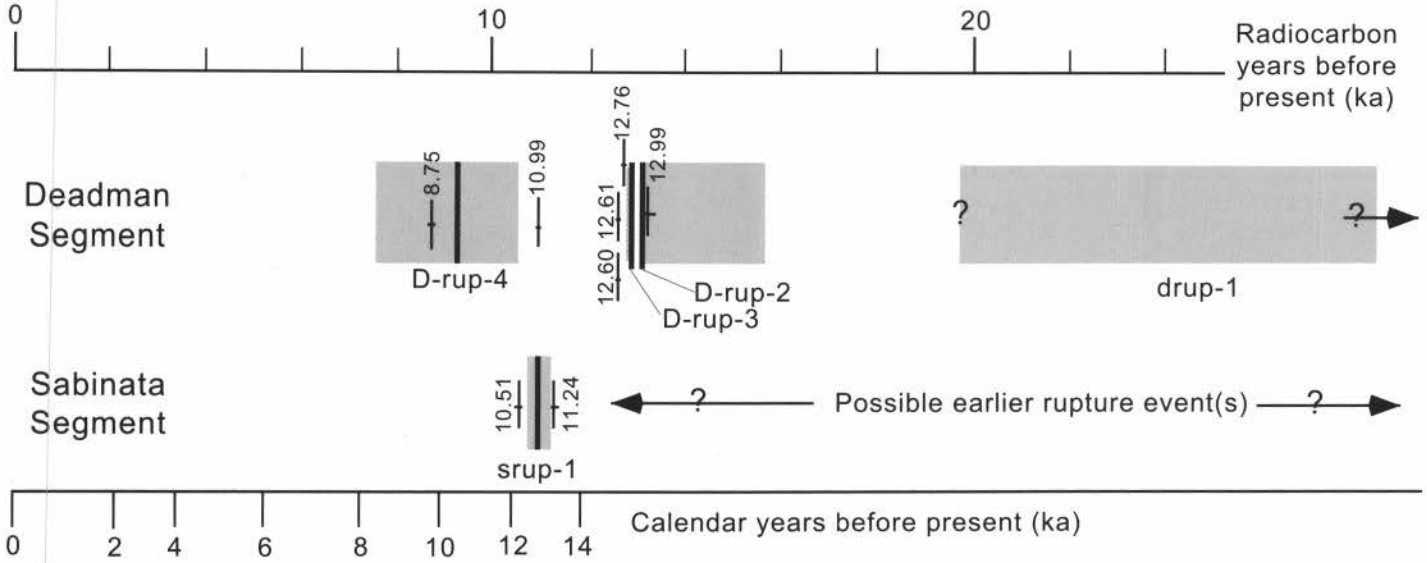

FIGURE 7. Interpreted timing of rupture events on the studied portion of the Alamogordo fault. Thick vertical lines indicate preferred dates of ruptures. Labeled vertical tics give C-14 age constraints in thousands of ^{14}C yrs B.P.; 1 sigma laboratory errors are shown as horizontal bars on the C-14 age constraints. Shaded intervals indicate the possible range in the timing of a specific rupture. Age range of D-rup-4 is based on the interpreted age range of map unit Qf2; the C-14 date of 8,750 ^{14}C yrs B.P is from a debris flow in Qf2 (Koning et al., this volume). Queries on the ends of the shaded intervals emphasize uncertainty. Relationship of C-14 ages to calendar ages obtained from Stuiver and Becker (1993) and Beta Analytic Inc. for <8000 calendar years before present; relationships after 8000 yr based on Becker and Kromer (1993) and Bard et al. (1990).

developed below the upper contact of the unit in calcareous sediment. Unit C2a sharply overlies C1 and is only about 1 m long and 20-35 cm thick. It also has a wedge shape and is composed of poorly sorted, matrix-supported pebbles and cobbles with no discernable fabric. The clasts in unit C2a have an 80-100 % coverage by <0.3 mm-thick coats of carbonate and gypsum. Unit C2b is unique in that it contains clast-supported boulders and cobbles with loose sandy clay loam between the clasts. Charcoal

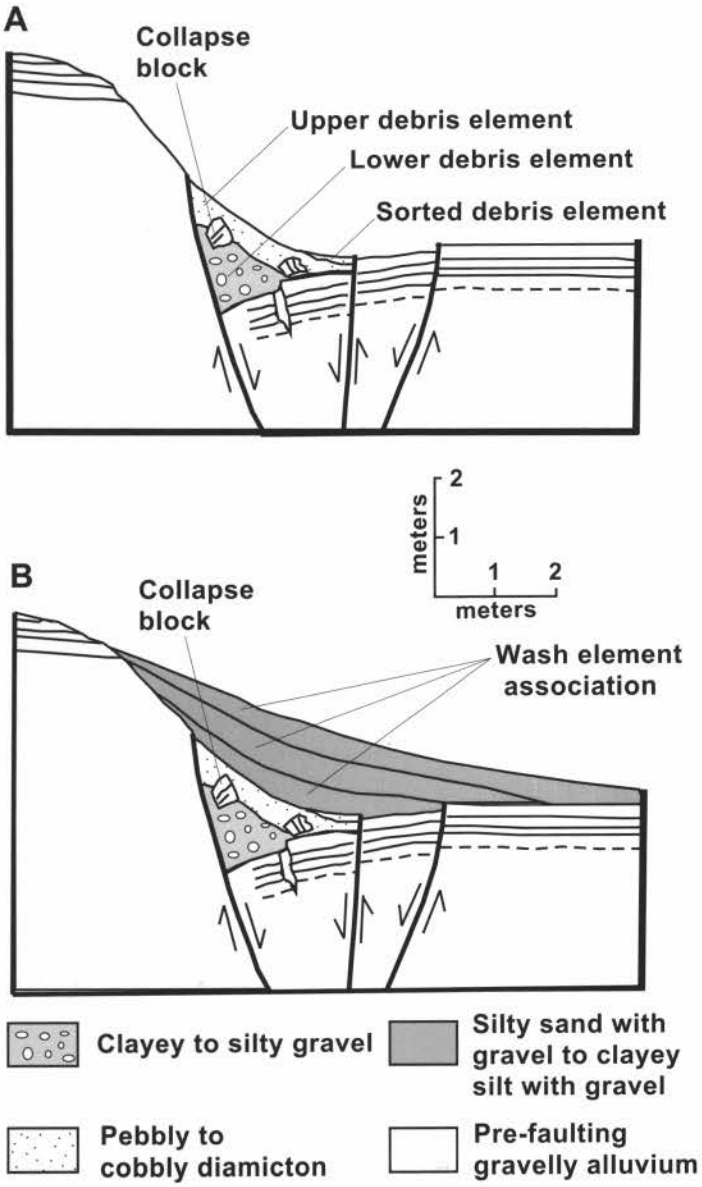

FIGURE 8. Sequential diagrams illustrating architectural elements of fault-scarp colluvium following a hypothetical 2.2 m displacement on a normal fault in gravelly alluvium (modified from Nelson, 1987 and 1992). A) Debris element. B) Wash element. See Table 1 for characteristics of a particular colluvium architectural element.

and snail shells, which are relatively common in the sandy clay loam matrix, yielded C-14 dates of 12,600 ± 80 ^{14}C yrs B.P. and 12,760 ± 50 ^{14}C yrs B.P. (samples Beta-117016 and -119269). Unit C2c is thick, sharply overlies all of the underlying colluvial units, and is marked by distinct beds sloping 30-35° away from the fault scarp. The clast fabric parallels the inclined bedding, suggesting deposition on an inclined colluvial slope. Unit C2c is also wedged-shaped, and the lower distal part of the unit has a distinct, well sorted, clast-supported, open-framework of coarse pebbles with very little matrix (probably corresponding with the sorted debris element, Fig. 8). C-14 dating of snail shells returned a value of 12, 610± 40 ^{14}C yrs B.P. (sample Beta-119268). A soil developed on the upper distal part of this unit has weak structural development with few, faint to distinct, clay films. Unit C2d has a gradational lower contact and is composed of matrix-supported cobbles and pebbles. Unit C2e has about 65% matrix, a tabular shape, a gradational lower contact, and no clast fabric or sedimentary structures.

Virtually all of the late Quaternary displacement at this locality has occurred along a loose, 10-40 cm-wide shear zone labeled Flt1 (Fig. 10). Within this zone, clasts show a strong vertical alignment due to shear rotation. This shear zone extends to the top of unit C1. Although a fracture (Fr3 in Fig. 10) extends up into unit C2a, the top contact of C2a is not noticeably offset. However, on the right margins of C2c and C2a there is evidence of a minor shear zone (Flt3) based on subvertical clast alignment, interpreted to reflect clast rotation, and a down-warped colluvial gravel bed (Fig. 10). Another shear zone (Flt2 in Fig. 10) lies below unit A1'.

Paleoseismic Interpretation:

One large rupture event occurred after the deposition of unit A2 and after enough time to allow a stage II to II+ carbonate morphology to develop in the soil on A2. During or immediately following this rupture event, a block of sediment comprising units A1' and A2' fell from the top of the newly created, near-vertical, free scarp face to the top of unit A2 in the hanging wall (Figs. 10-11). An alternative hypothesis is that unit A2' was only deposited in the hanging wall, perhaps in response to an earlier rupture event, and that unit A1' fell alone. However, the lower beds of unit A2' are generally parallel (albeit somewhat deformed) with the upper soil and bedding of unit A1' (Fig. 10), suggesting that unit A2' was initially deposited on top of non-deformed, subhorizontal strata of unit A1' on the immediate footwall. Consequently, we interpret that A1' and A2' fell as a relatively cohesive block due to well developed Bk and Bt soil horizons (particularly in unit A1); this collapse phenomena has been observed along the La Jencia fault (Machette, 1988, log of trench 3). The block rotated as it fell so that its beds were somewhat vertical when it landed. Unit A2 predates this rupture event because it was deformed by it. Thus, the maximum time constraint for this rupture event appears to be 13 ka radiocarbon years, as determined from the C-14 date on charcoal in the Bt soil horizon of A2' (Fig. 10). This assumes that the charcoal did not get mixed in with the Bt horizon during the topple of the block or somehow mixed in by later colluvial deposition or bioturbation.

Colluvium C1a overlies A1' and A2'. The shape and sedimentologic character of C1a corresponds very well with the lower debris architectural element of Nelson (1992) (Table 1). For example, unit C1a is wedge-shaped and deposition appears to be controlled by gravity (it lacks clast fabric and is poorly sorted), but surface wash deposition may be partly responsible for its vague bedding and its upper calcareous sediment. Unit C1a also directly abuts the fault scarp and has a sharp lower contact over the fallen blocks of sediment A1' and A2'.

The discontinuous calcareous sediment on top of unit C1a has undergone minor pedogenesis, as is evident by its weak soil structure and faint clay films, but its calcium carbonate enrichment may at least partly be due to sedimentation processes. During

TABLE 1. Architectural elements for colluvium derived from a fault scarp.+

Element	Location & time of deposition*	Diagnostic features	Texture	Depositional process
Lower Debris	Directly abuts the fault. Rapid (50-1000 yr)	Wedge-shaped; thickens towards fault. Sharp lower contact. Large collapse blocks of soil or sediment. Stratification and oriented clasts are rare.	Boulders, cobbles, & pebbles with subordinate loose matrix of silt or clay.	Gravity (falling, toppling, slumping, or sliding of sediment blocks); surface wash and eolian deposition are minor. Equidimensional blocks or clasts may slide or roll down previously deposited colluvium and accumulate near toe of the wedge.
Upper Debris	Overlies lower debris element. Rapid (50-2,000 yr)	Compared to lower debris element: thinner, more laterally extensive, and finer-grained. May contain small lenses of sand or fine gravel Mostly matrix-supported	Diamicton: hetereogeneous mixture of matrix and gravel.	Both gravitational as well as wash and creep processes are important.
Wash	Overlies and extends beyond debris element; overlaps eroded free face of scarp . Gradual (10^2 to 10^5 years)**	Subtabular shape. Non-stratified and bioturbated Gradational lower contact	Silty sand to clayey silt with low amounts of gravel.	Rainsplash, sheetwash and rillwash.

+ Assumes fault scarp formed in gravelly alluvium; modified from Nelson (1992)

* Location is within fault scarp colluvium derived from a single rupture event. Time is from Wallace (1977); M.N. Machette, pers. comm., 2002; Machette and Crone, 2001; and modern observations of 1915 Pleasant Valley fault scarp and 1954 Fairview Peak fault scarp (J. McCalpin, pers. comm., 2002).

** Note that the time range is highly dependent on texture and cohesion of the uplifted parent materials as well as climatic and environmental factors.

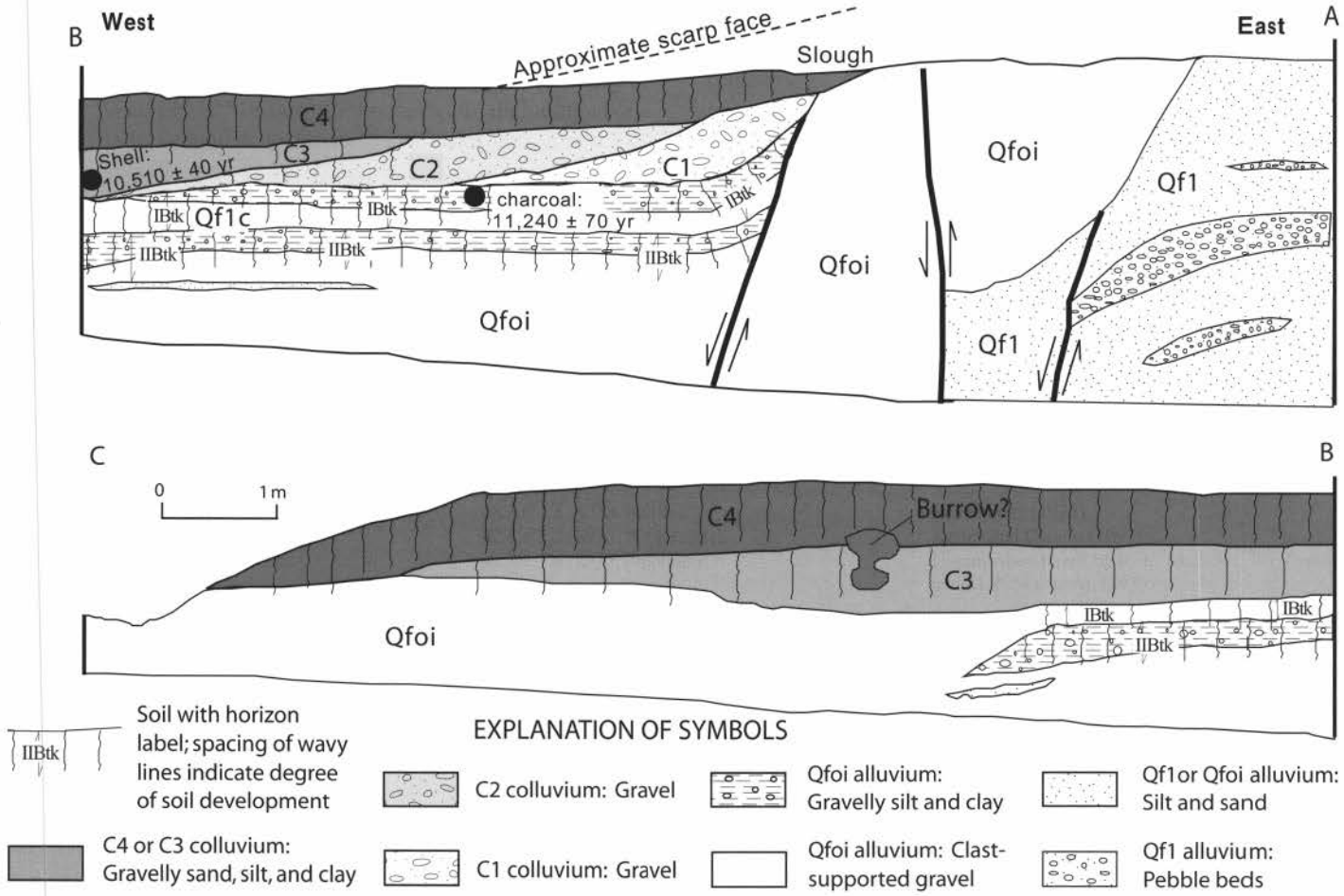

FIGURE 9. Lab-1 exposure. Brief descriptions of sediment units are in text; full descriptions are in Koning (1999). C-14 dates listed next to dark circles are in radiocarbon years. Thick black lines indicate fault strands; arrows show relative motion. Located at N: 3,652,820±30 m, E: 412,005±30 m (UTM zone 13, NAD 27).

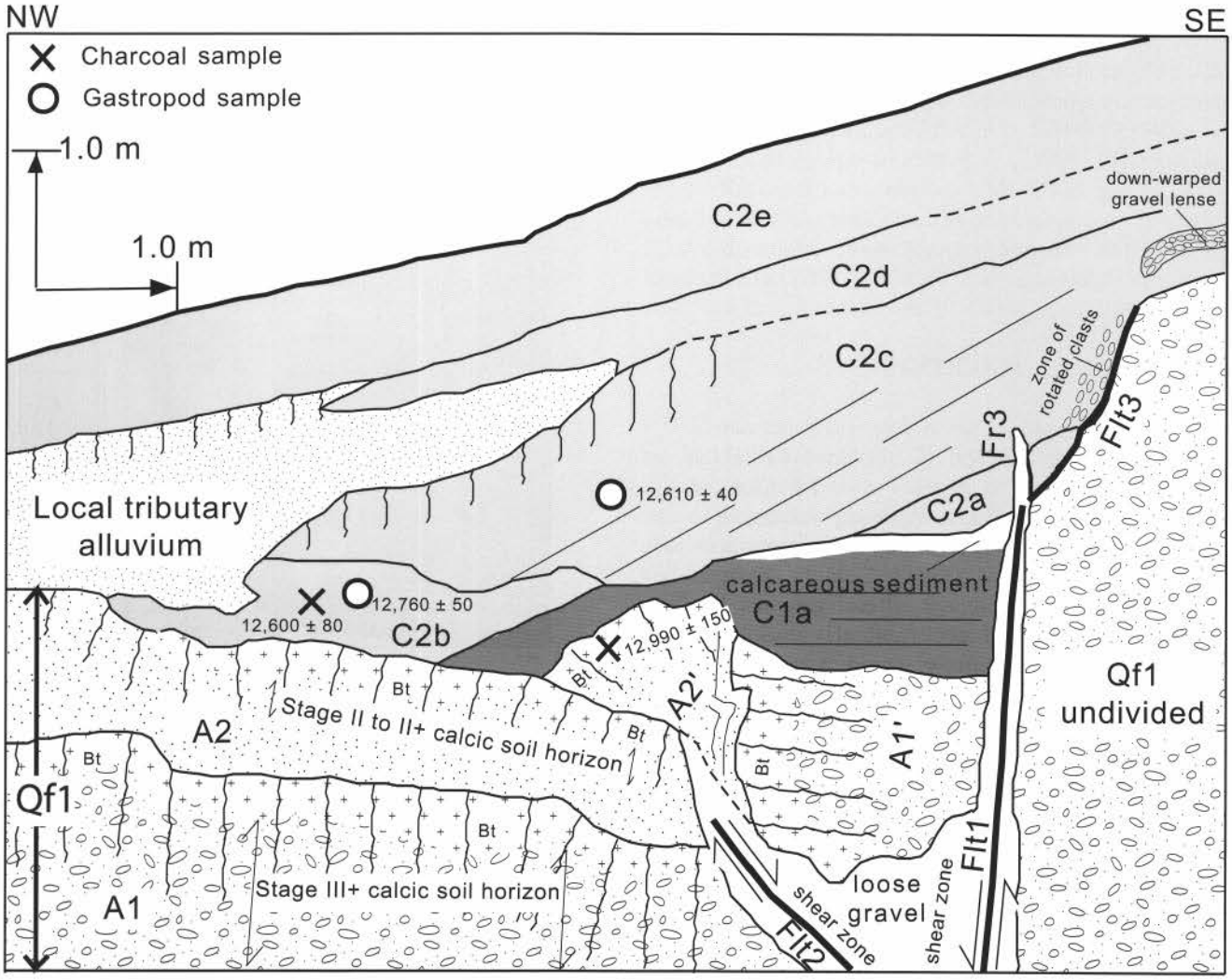

FIGURE 10. M-19 exposure. Circles and X's are locations of sampled gastropod shells and charcoal (respectively) for C-14 dating. Numbers next to sample locations are radiocarbon dates reported in ^{14}C yrs B.P. Fault strands labeled Flt1, Flt 2, and Flt3; fracture labeled as Fr3. Straight, short lines schematically illustrate bedding; two detailed bedding contacts are drawn at base of unit A2' to illustrate stratigraphic relationship of A1' to A2'. Wavy lines denote buried soils; these lines do not mark depth of soil. A1 and A2 are Qf1 alluvial units that have well developed soils. The pattern composed of small crosses, labeled "Bt," marks prominent Bt soil horizons in units A1 and A2; these are underlain by calcic horizons. A1' and A2' correspond to blocks of units A1 and A2 that have toppled from a former fault scarp free face immediately following a rupture event. Units C1a and C2a through C2e are colluvium derived from the adjacent fault scarp. Local tributary alluvium is derived from arroyo to the northeast and may correlate to unit Qf2. Brief descriptions of units in text; full descriptions given in Koning (1999). Located at N: 3,634,560±30 m, E: 412,980±30 m (UTM zone 13, NAD 27).

erosion of the fault scarp, erosion of units A1 and A2 (which probably were located on the fault scarp shoulder; Fig. 11) would have resulted in the transport and deposition of calcareous sediment at the foot of the fault scarp. A component of this calcareous sediment may also have been derived from eolian processes.

A second rupture probably occurred within 2,000 years after the first event because of the lack of a wash element in unit C1a (except for possibly the thin, discontinuous body of calcareous sediment). The lower and upper debris elements, which are associated with a scarp free face, are generally covered by the wash element after the free face has been buried (Fig. 8) (Nelson, 1992). The time that it takes to bury a free face, and thus presumably transition from the debris element to the wash element, is probably no more than 1,000-2,000 years, depending on the size of the free face, the nature of the sediment, and the climate (Wallace, 1977; Machette and Crone, 2001; M.N. Machette, personal commun., 2002).

This second event formed a graben at the foot of the fault scarp, and all of unit A1' and part of unit A2' dropped into this graben (Fig. 11). Dropping of these blocks rotated the beds of the southeastern (i.e., proximal) part of unit C1a from a pre-rupture inclined position to a post-rupture near-horizontal position (Figs. 10 and 11).

Unit C2a is interpreted as a collapse deposit from the fault scarp free face formed by the second rupture event because of its heterogeneous clast orientations, carbonate-coated clasts, wedge shape, and poor sorting. The carbonate-coated clasts are likely to have been derived from a wedge of C1a that was deposited across the fault trace following the first rupture; this wedge then fell off the fault scarp free face immediately after the second rupture.

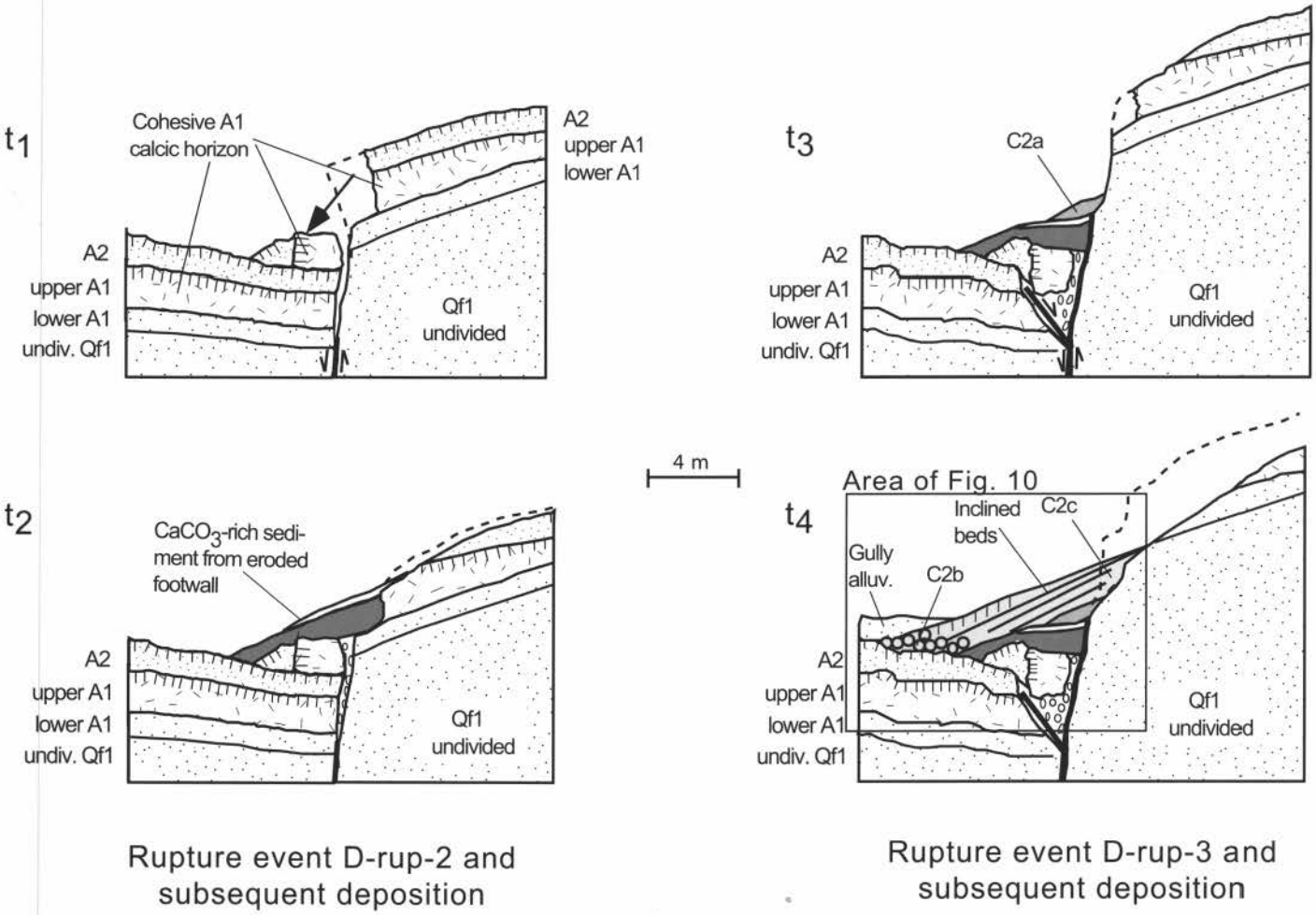

FIGURE 11. Interpreted fault scarp degradation and colluvial deposition at site M-19 prior to deposition of units C2d and C2e (not shown). Each block diagram illustrates successive time intervals labeled t_1 through t_4 (oldest to youngest, respectively). t_1 = immediately after D-rup-2; t_2 = deposition of lower and upper C1a; t_3 = faulting (D-rup-3) and subsequent deposition of C2a; t_4 = deposition of units C2b and C2c. Dashed line indicates portion of surface from earlier time interval that was later eroded.

Following the second rupture, units C2b and C2c were deposited as the lower debris element and mixed lower/upper debris elements, respectively (Fig. 11). Three C-14 dates from charcoal and snail shells within these units yielded ages between 12,500 and 12,800 radiocarbon years; these provide a minimum time constraint for the second rupture. Evidence for reworking of soil from the footwall includes minor clay films on clasts and 50-100 % coverage of clasts by carbonate coats (≤ 0.4 mm-thick) (Koning, 1999). A weak 30-cm-thick soil formed on the northwest, distal top of C2c (Fig. 10). This soil was buried by local tributary alluvium and then by more colluvium. Unit C2d is interpreted to represent an upper debris element (Table 1). The deposition of C2d was probably a response to a change in stability of the fault scarp face due to environmental or climatic factors because the youngest fault strand, Flt3, does not appear to break the top of the C2c unit (Fig. 10). Lastly, unit C2e was deposited over a relatively long time period (thousands of years) and represents a wash element (Table 1).

In summary, we interpret two large-displacement rupture events based on the local stratigraphy and following the concepts of fault scarp colluvium architectural elements (Nelson, 1992). These rupture events probably occurred within about 1000-2000 years prior to deposition of colluvium dated at 12.5-12.8 ka (radiocarbon years) and are referred to as D-rup-2 and D-rup-3 (Fig. 7). The primary reasons that we do not interpret one large event are: (1) the horizontal bedding of C1a abuts Qf1 deposits in the footwall across a near-vertical fault, and (2) these horizontal beds were probably initially inclined to the west, like the beds of the colluvium above, and later rotated into their present position by a second rupture event.

Considering the thickness of fault scarp-derived colluvium and the 7.8 m of surface offset at M-19, as measured from the projected top of Qf1 (Koning, 1999), throw associated with D-rup-2 and D-rup-3 can be estimated if one assumes that these rupture events created most of the fault scarp at M-19 and subunits A1 and A2 were initially present on either side of the fault. Assuming that A1 pre-dates the formation of the modern fault scarp is consistent with: (1) sedimentologic similarities between unit A1 and uppermost Qf1 sediment on the footwall (Koning, 1999, appendix C), and (2) an average imbrication direction of

A1 indicating a paleoflow directly away from the mouth of the canyon (Koning et al., this volume). An A2' equivalent is not presently observed in the footwall, but because the lower beds of unit A2'approximately parallel the top of unit A1' it is interpreted that both fell from the footwall onto the hanging wall (Fig. 10). Either unit A2' was later eroded from the top of the fault scarp (Fig. 11), or its initial deposition in the footwall was only adjacent to the fault exposed at site M-19. Units A1', A2', and C1a filled in about 2 m of space (Fig. 10). Assuming these units buried the scarp free face, this suggests an approximate throw of 2 m for D-rup-2 (Fig. 11). Erosion of the fault scarp face following D-rup-3 resulted in a voluminous amount of colluvium associated with C2a through C2e (~3 m-thick), and thus D-rup-3 probably had a higher throw (estimate 3 to 6 m, or 1 to 2 times the colluvial thickness) (Fig. 11). These throw values are comparable to the 4-5 m maximum displacement interpreted for the Organ fault on the southeastern side of the Tularosa Basin (Gile, 1987) and other Basin and Range faults (DePolo et al., 1991). Having two rupture events with these throw values can account for much of the surface offset (generally 3-11 m for offset Qf1 surfaces; Koning, 1999) observed on fault scarps associated with the Alamogordo fault (e.g., eastern fault scarp in Fig. 5).

A down-warped gravel lens and a zone of rotated clasts on the southeast margin of unit C2c (Fig. 10) may be due to a small rupture event (probably D-rup-4) that created a minor shear zone in unit C2c but did not create a significant fault scarp free face.

DISCUSSION OF FAULT ACTIVITY AND SEISMIC HAZARDS

Fault Segmentation

As many as five rupture events in the latest Pleistocene to early Holocene (30-7.5 ka) are interpreted along the Alamogordo fault and referred to as S-rup-1 and D-rup-1 to -4 (Fig. 7). The youngest rupture event in the northern study area (S-rup-1), based on data from the Lab-1 outcrop, occurred at a different time than the four ruptures interpreted from data south and east of Alamogordo (D-rup-1 to –4), including the M-19 outcrop (Fig. 7). This timing difference is consistent with the interpretation that two fault segments exist in the study area, with their common segment boundary (Alamogordo Boundary Zone) being near Alamogordo (Fig. 1). This segmentation interpretation is further supported by numerous morphometric, geologic, and geophysical data presented and discussed in Koning (1999). Rupture D-rup-3 may have involved both segments because of its large inferred displacement (3-6 m) at site M-19. However, there is presently no evidence at the Lab-1 exposure confirming that D-rup-3 occurred on the Sabinata segment.

These two fault segments may possibly explain the close timing of ruptures D-rup-2 and D-rup-3 at site M-19. For example, one of the ruptures may have initiated on one segment and partly spilled over into the adjoining segment, as observed in the Borah Peak earthquake of 1983 (DePolo et al., 1991). This spill-over may have strained the adjoining segment sufficiently to initiate a second rupture soon after the first.

Magnitudes of Late Quaternary Earthquakes on the Alamogordo Fault

The magnitudes of late Quaternary earthquakes associated with surface rupture events in the study area were estimated using published empirical relationships between moment magnitude (Mw) and rupture displacement along with moment magnitude (Mw) and rupture length (Wells and Coppersmith, 1994) (Table 2). The rupture length was approximated using paleoseismic data discussed in this chapter and the straight-line lengths of the Deadman and Sabinata segments (Fig. 1). The segment length includes the straight-line length of the fault within the Alamogordo Boundary Zone up to the west-pointing corner of the mountain front northeast of Alamogordo. Events D-rup-4 and S-rup-1 are interpreted to be confined to the Deadman and Sabinata segments, respectively, and part of the Alamogordo Boundary Zone, because these ruptures did not occur simultaneously (Fig. 7). Event D-rup-3 is assumed to involve both segments, which is not unusual for large-displacement earthquakes (e.g., DePolo et al., 1991), and the Mw estimated using the fault length of both segments is compatible with Mw values estimated using displacement values. Mw was also calculated directly using the definition of seismic moment (Mo) by estimating the seismogenic depth, rupture length, average displacement, and average fault dip at depth (Table 2). According to these various procedures, the Alamogordo fault is capable of producing earthquakes with moment magnitudes of 6.7-7.3. However, these moment magnitude values are subject to change based on future study.

Late Quaternary Slip Rates on the Alamogordo Fault

The occurrence of as many as five latest Pleistocene-early Holocene ruptures may represent a temporal earthquake-clustering event preceded by lesser earthquake activity during the late Pleistocene (30-130 ka) on the studied portion of the Alamogordo fault. Earthquake clustering is a bimodal distribution of earthquake recurrence that has been inferred for other faults in the Rio Grande rift and Basin and Range (Machette, 1987b; McCalpin, 1996). Temporal earthquake clustering along the Alamogordo fault is discussed in Koning (1999).

Calculating late Quaternary slip rates using a surface offset value of 5-7 m (5 m average surface offset for modern fault scarps plus 2 m for possible previous scarp erosion and burial) yields a minimum rate of 0.04-0.05 mm/yr and a maximum rate of 0.17-0.23 mm/yr. The minimum rate assumes tectonic quiescence over the late Pleistocene (30-130 ka), prior to latest Pleistocene temporal clustering, and a time value of 130,000 yrs. The maximum rate assumes that displacement rates interpreted over the past 30,000 yrs characterize the late Quaternary (i.e., time value of 30,000 yrs). These rates generally fall within the broad <0.2 mm/year slip rate category shown by Machette et al. (1998) for most faults in New Mexico (including the Alamogordo fault).

Implications for Seismic Hazards

The Alamogordo fault is a 110 km long structure (end-to-end) that extends along the base of the Sacramento Mountains. The

TABLE 2. Seismic data for late Quaternary surface rupture events along the Alamogordo fault.

Rupture event	Segment[1]	Rupture length (km)[1]	Estimated maximum displacement (m)	Estimated average displacement (m)	Moment Magnitude (Mw) from rupture length[2]	from max. displacement (m)[2]	from average displacement (m)[2]	Estimated depth of rupture (km)[3]	Calculated Mo (x1026)[4]	Calculated Mw[4]
D-rup-1	D(?)	32	2.5	1.3	6.8	6.9	6.8	16	2.0	6.8
D-rup-2	D(?)	32	3	1.5	6.8	6.9	6.9	16	2.3	6.9
D-rup-3	D & S	63	6	3	7.2	7.2	7.1	16	9.1	7.3
D-rup-4	D	32	1.5	0.8	6.8	6.7	6.7	16	1.5	6.7
S-rup-1	S	31	3	1.5	6.8	6.9	6.9	14	2.0	6.8

Notes:

1 D= Deadman segment; S = Sabinata segment. Refer to Koning (1999) for discussion of fault segments and segment boundaries.

2 Mw (moment magnitude) estimated using regression equations for normal faults (Tables 2A and 2B of Wells and Coppersmith, 1994).

3 Estimated depth of rupture was obtained using the theoretical height of the seismogenic layer that is calculated using the spacing of the main antithetic fault from the master half-graben fault. This gives the width of the half-graben. The location of the antithetic fault was placed where there was a steep bouguer gravity anomally east of the Tres Hermanos Hills (Koning, 1999, figure 33). According to Scholz and Contreras (1998): theoretical height of seismogenic layer = (width of half-graben) / (cot (dip of fault)). We assume that earthquakes on the Alamogordo fault nucleate near the base of the seismogenic layer (Das and Scholz, 1983; Scholz, 1990).

4 Moment magnitude (Mw) was calculated by the equation: Mw = (log(Mo) - 16.05)/1.5 (Hanks and Kanamori, 1979), where Mo= mAD. m = shear modulus = 3 x 1011 dyne/cm2 (Yeats et al., 1997); A= rupture length x estimated rupture depth; D = average displacement.

Alamogordo fault in the study area is interpreted to have ruptured the surface 3-5 times during the latest Pleistocene through early Holocene, depending on location and the uncertainty regarding the number of events on the Sabinata segment. These surface rupture events, each having an estimated average of 1-3 m of displacement, produced as much as 10 m in cumulative surface offset in unit Qf1. The last rupture on the Deadman segment occurred in the early Holocene during the aggradation of unit Qf2. Thus, the Alamogordo fault should be considered an active fault capable of producing 6.7 through 7.3 moment magnitude earthquakes (Table 2) on at least two fundamental seismogenic fault segments.

ACKNOWLEDGMENTS

The senior author would like to thank his M.S. committee members Frank Pazzaglia, Les McFadden, Karl Karlstrom, and Mousumi Roy for their advice and guidance during this study. Others who contributed important information or comments include Michael Machette, John Hawley, Jon Geissman, Joel Pederson, Missy Eppes, and James McCalpin. We gratefully acknowledge the field assistants who helped make this work possible: Sheila Hutchinson, Jessy Preston, Karl Wegmann, Emily Repanich, Jasper Shaer, Jen Ortega, and Dave Mitchell. Funding for the project was provided by the University of New Mexico Research Project and Travel grant (RPT), Geological Society of America Research Grant 6270-98, Geological Society of America Howard Award, New Mexico Geological Society, Geology Alumni Scholarship Fund (University of New Mexico), Jean-Luc Miossec Memorial Scholarship, and the Federal Emergency Management Agency (FEMA). The manuscript was improved by the reviews of James McCalpin and Michael Machette.

REFERENCES

Bard, E., Hamelin, B., Fairbanks, R.G., and Zindler, A., 1990, Calibration of the C-14 timescale over the past 30,000 years using mass spectrometric U-Th ages from Barbados corals: Nature, v. 345, p. 405-410.

Becker, B., and Kromer, B., 1993, The continental tree-ring record – absolute chronology, C-14 calibration and climate change at 11 ka: Palaeogeography, Palaeoclimatology, Palaeoecology, vol. 103, p. 67-71.

Birkeland, P.W., 1999, Soils and geomorphology: New York, Oxford University Press, 430 p.

Bucknam, R.C., and Anderson, R.E., 1979, Estimation of fault scarp ages from scarp height — slope angle relationship: Geology, v. 7, p. 11-14.

Das, S., and Scholz, C.H., 1983, Why large earthquakes do not initiate at shallow depths: Nature, v. 305, p. 621-623.

DePolo, C.M., Clark, D.G., Slemmons, D.B., and Ramelli, A.R., 1991, Historical surface faulting in the Basin and Range province, western North America: implications for fault segmentation: Journal of Structural Geology, v. 13, p. 123-136.

Folk, R.L., 1954, The distinction between grain size and mineral composition in sedimentary rock nomenclature: Journal of Geology, v. 62, p. 344-359.

Gile, L.H., 1987, Late Holocene displacement along the Organ Mountains fault in southern New Mexico: New Mexico Bureau of Mines and Mineral Resources, Circular 196, 43 p.

Hanks, T.C., and Kanamori, H., 1979, A moment magnitude scale: Journal of Geophysical Research, v. 84, p. 2348-2350.

Kelley, V.C., and Thompson, T.B., 1964, Tectonics and general geology of the Ruidoso-Carrizozo region, central New Mexico, Ruidoso Country: New Mexico Geological Society, 25th Field Conference, Guidebook, p. 110-121.

Koning, D.J., 1999, Fault segmentation and paleoseismicity of the southern Alamogordo fault, southern Rio Grande rift, New Mexico [M.S. thesis]: Albuquerque, University of New Mexico, 286 p.

Machette, M.N., 1987a, Preliminary assessment of paleoseismicity at White Sands Missile Range, southern New Mexico — Evidence for recency of faulting and repeat intervals for major earthquakes in the region: U. S. Geological Survey, Open-file Report 87-444, 46 p.

Machette, M.N., 1987b, Changes in long-term versus short-term slip rates in an extensional environment; *in* Crone, A.J., and Omdahl, E.M., eds., Proceedings of Conference XXXIX – Directions in Paleoseismology: U. S. Geological Survey, Open-file Report 87-673, p. 228-238.

Machette, M.N., 1988, Quaternary movement along the La Jencia fault, central New Mexico: U.S. Geological Survey Professional Paper 1440, 82 p.

Machette, M.N., Personius, S.F., Kelson, K.I., Haller, K.M., and Dart, R.L., 1998, Map and data for Quaternary faults and folds in New Mexico: U.S. Geological Survey, Open-file Report 98-521, p. 181-185.

Machette, M.N., and Crone, A.J., 2001, Stop B3 — Late Holocene faulting on the Old Ghost alluvial-fan complex; *in* Machette, M.N., and others, eds., Quaternary and late Pliocene geology of the Death Valley region: Recent observations on tectonics, stratigraphy, and lake cycles (Guidebook for the 2001 Pacific Cell — Friends of the Pleistocene Fieldtrip): U.S. Geological Survey, Open-file Report 01-51, p. B67-B75.

McCalpin, J.P., 1996, Application of paleoseismic data to seismic hazard assessment and neotectonic research; *in* McCalpin, J. P., ed., Paleoseismology: San Diego, Academic Press, 588 p.

Nelson, A.R., 1987, A facies model of colluvial sedimentation adjacent to a single-event normal-fault scarp, Basin and Range province, western United States, *in* Crone, A.J., and Omdahl, E.M., eds., Directions in Paleoseismology – Proceedings of Conference XXXIX: U.S. Geological Survey, Open-file Report 87-673, p. 136-145.

Nelson, A.R., 1992, Lithofacies analysis of colluvial sediments – An aid in interpreting the recent history of Quaternary normal faults in the Basin and Range Province, western United States: Sedimentary Petrology, v. 62, p. 607-621.

Otte, C., Jr., 1959, Late Pennsylvanian and Early Permian stratigraphy of the northern Sacramento Mountains, Otero County, New Mexico: New Mexico Bureau of Mines and Mineral Resources, Bulletin 50, 111 p.

Oviatt, C.G., Currey, D.R., and Sack, D., 1992, Radiocarbon chronology of Lake Bonneville, eastern Great Basin, U.S.A.: Palaeogeography, Palaeoclimatology, Palaeoecology, v. 99, p. 225-241.

Pray, L.C., 1961, Geology of the Sacramento Mountains Escarpment, Otero County, New Mexico: New Mexico Bureau of Mines and Mineral Resources, Bulletin 35, 144 p.

Scholz, C.H., 1990, The mechanics of earthquakes and faulting: Cambridge, Cambridge University Press, 439 p.

Scholz, C.H., and Contreras, J.C., 1998, Mechanics of continental rift architecture: Geology, v. 26, p. 967-970.

Soil Survey Staff, 1992, Keys to Soil Taxonomy: Soil Conservation Service Technical Monograph No. 19, 5th ed., 541 p.

Stuiver, M., and Becker, B., 1993, High-precision decadal calibration of the radiocarbon time scale, AD 1950-6000 BC: Radiocarbon, v. 35, p. 35-65.

Wallace, R.E., 1977, Profiles and ages of fault scarps, north-central Nevada: Geological Society of America Bulletin, v. 88, p. 1267-1281.

Wells, D.L., and Coppersmith, K.J., 1994, Empirical relationships among magnitude, rupture length, rupture area, and surface displacement: Bulletin of the Seismological Society of America, v. 84, p. 974-1002.

Yeats, R.S., Sieh, K., and Allen, C.R., 1997, The geology of earthquakes: New York, Oxford University Press, 568 p.

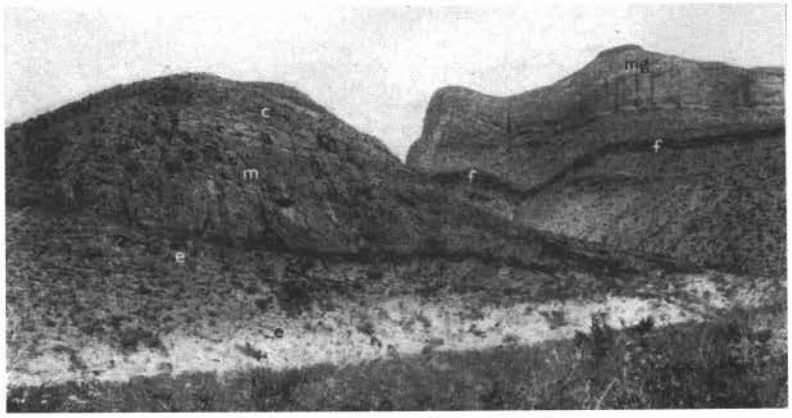

North side of entrance to Alamo Canyon three miles south of Alamogordo. Symbols: Mg – Magdalena (Madera) Group; f – Fusselman group; c – cherty member of the Montoya limestone; m – massive member of Montoya Formation; e – El Paso Formation. Photo from Darton (1928). This photo was taken in the vicinity of the Alamogordo Fault, the subject of a neotectonic study by Koning and Pazzaglia (this volume).